Separation Science and Technology
Publication details, including instructions for authors and subscription information:
http://www.informaworld.com/smpp/title~content=t713708471

Recovery of 1,4-Dimethyl Piperazine from Aqueous Solutions Using Polymeric Adsorbent and Ion-Exchange Resins

Kiran P. Akre[a]; Vilas G. Gaikar[a]
[a] Institute of Chemical Technology, University of Mumbai, Matunga, Mumbai, India

To cite this Article Akre, Kiran P. and Gaikar, Vilas G.(2006) 'Recovery of 1,4-Dimethyl Piperazine from Aqueous Solutions Using Polymeric Adsorbent and Ion-Exchange Resins', Separation Science and Technology, 41: 8, 1593 — 1617
To link to this Article: DOI: 10.1080/01496390600674810
URL: http://dx.doi.org/10.1080/01496390600674810

Separation Science and Technology, 41: 1593–1617, 2006

ISSN 0149-6395 print/1520-5754 online
DOI: 10.1080/01496390600674810

Recovery of 1,4-Dimethyl Piperazine from Aqueous Solutions Using Polymeric Adsorbent and Ion-Exchange Resins

Kiran P. Akre and Vilas G. Gaikar
Institute of Chemical Technology, University of Mumbai, Matunga,
Mumbai, India

Abstract: Strong and weakly acidic ion exchange resins and polymeric adsorbents are used for recovery of 1,4-dimethyl piperazine (DMP) from aqueous solutions. Sorption of the amine in undissociated form is the primary mechanism of uptake of DMP on the ion-exchange resins. Equilibrium adsorption data for DMP on the resins, at various temperatures, are fitted in Langmuir adsorption isotherm. Kinetic studies show that intraparticle diffusional resistance controls the sorption of DMP into the resin matrix. A mathematical model based on intraparticle diffusion and external mass transfer is used for simulating breakthrough profiles and compared with the experimental results for a fixed bed of weakly acidic Indion-652 resin. The DMP loaded bed of the resin was effectively regenerated with methanol.

Keywords: 1,4-Dimethyl piperazine, sorption, adsorption, ion-exchange resins, Langmuir isotherm, break-through curve, recovery

INTRODUCTION

Heterocyclic amines, such as piperazine, morpholine, quinoline, pyridine, etc. are toxic pollutants that exist in the effluents of various major industries (1). Besides being the source of pollution, there is a loss of valuable chemicals. The development of separation processes, therefore, to recover such chemicals has become increasingly important. Adsorption of these amines

Received 1 September 2005, Accepted 15 February 2006

Address correspondence to Vilas G. Gaikar, Institute of Chemical Technology, University of Mumbai, Matunga, Mumbai 400 019, India. Fax: 91-22-24145614. E-mail: v.g.gaikar@udct.org

on activated carbon (2, 3), activated sludge (4, 5), cation exchange resins (6) and polymeric adsorbent resins (7) has been reported in the literature. Activated carbon has a good adsorption capacity for the amines but the carbon loaded with these solutes is difficult to regenerate with simple processes because of strong molecular interactions with a variety of polar groups on the surface of activated carbon (8).

Polymeric adsorbents have a potential for such separations, particularly for separation/recovery of hydrophobic organic molecules from the aqueous solutions (9). However, for highly water soluble organic solutes the adsorption capacity can be poor. The presence of functional group on the polymeric structure should help in improving the efficiency of such adsorbents. Ion exchange resins with acidic groups can function as a mass separating agent for separation/recovery of basic compounds from aqueous solutions. Neutralization reaction between the basic compound and the acidic group on polymeric resin can provide the necessary separation principle.

1,4-Dimethyl piperazine (DMP), an intermediate in pharmaceutical industry, is produced by alkylation of piperazine and is a highly water soluble amine. A common method of its separation from water is conversion into a salt by addition of a mineral acid. Water is then evaporated from the non-volatile salt. Obviously, a large amount of water needs to be evaporated and further DMP needs to be recovered from the salt by an alkali treatment, increasing the overall cost of operation and producing a salt which may not always have any significant economical value. The separation of DMP from aqueous solutions is attempted in this work using acidic ion exchange resins containing strongly acidic $-SO_3H$ and weakly acidic $-COOH$ groups and also with a non-polar polymeric adsorbent resin for comparison. The interaction between the acidic hydrogen of the resin and nitrogen of the amine group of DMP is responsible for the uptake of the amine by the acidic ion exchange resins. The protonated amine may remain attached to the anionic stationary charge of the resin by electrostatic interactions. In the case of the non-ionic resin, the uptake of DMP is due to hydrophobic interactions and van der Waal forces. The removal of piperazine and its N-substituted diethyl derivatives from aqueous solutions by solvent extraction using a polar organic solvent has been reported in the literature (10).

Materials and Reagents

Pure DMP was purchased from Himedia, Mumbai and an industrial aqueous solution of DMP was available from Catapharma Ltd., Nashik, India. 1,4-Dimethyl piperazine is a weak base, with reported pKa values of 9.7 and 5.2 at 25°C (11). A weak cation exchange resin (Indion-652), a strong cation exchange resin (Indion-190), and a polymeric nonionic adsorbent (Indion NPA-I) were supplied by Ion Exchange (I) Ltd., Mumbai. Indion-652 is weakly acidic macroporous resin with polymethacrylate backbone and -COOH as the functional group attached to it. Indion 190 is a strongly acidic macroporous resin with $-SO_3H$ as the functional group. NPA-I is a non-ionic polymeric adsorbent. Both Indion-190 and NPA-I resins have a polystyrene backbone cross-linked with divinylbenzene. The detailed properties of resins are reported in Table 1. All solvents were of analytical grade.

EXPERIMENTAL

Conditioning of the Resins

The resins were first washed with 5% (w/v) aqueous solution of HCl, and the excess acid was removed by further washing the resin with a large volume of distilled water. The resins were then thoroughly washed with methanol and dried in an oven overnight at 330 K, and subsequently cooled to room temperature of 303 K before use.

Batch Adsorption Studies

The equilibrium adsorption isotherms were determined by contacting a known quantity of each of the resins (0.2–0.5 gm) with 10 cm^3 of aqueous solutions of DMP at different concentrations (0.1–0.4 mol/dm^3), in a stoppered flask. The flasks were kept on a mechanical shaker for a period of 3 hours which

Table 1. Properties of resins[a]

Properties	Indion-652	Indion-190	NPA-I
Type	Weak acid macroporous	Strong acid macroporous	Non functional polymeric adsorbent
Matrix structure	Polymethacrylic-divinyl benzene porous copolymer	Styrene-divinyl benzene copolymer	Styrene-divinyl benzene copolymer
Functional group	$-COOH$	$-SO_3H$	NA
Particle size (m) $\times 10^{-3}$	0.3–1.2	0.3–1.2	0.3–1.2
Ionic form	H^+	H^+	NA
Diameter of resin (mm)	0.75	0.75	0.75
Surface area (m^2/kg)	40×10^3	30×10^3	45×10^3
Exchange capacity (meq/kg dry resin)	3500	1900	NA
Internal voidage of resin	0.42	0.35	0.39
Elasticity parameter (η) (mol/cm^3) $\times 10^3$	3.11	3.36	3.22

[a] As provided by manufacturer of the resins.

NA: Not applicable.

was found by separate studies to be sufficient to reach the equilibrium. The residual concentration of the amine was determined by titration using standard aq. HCl solution and methyl orange as an indicator. The final pH of the solution and the volume changes of the resin due to sorption of water were also noted for each experiment. Each run was duplicated under identical experimental conditions with 4% error in reproducibility. The sorption capacity was determined from the solute mass balance, given the initial feed $(N_{LT})_f$ and final bulk (N_{LT}) concentrations. From the swelling of the resin, the *ab*sorbed quantity can be distinguished from the *ad*sorbed quantity, q (mol/kg dry resins). For the estimation of the *ab*sorbed amine in the swollen resin beads, it was assumed that the increased volume due to the swelling of the resins along with the pore volume is occupied by the solution having the same concentration as the external liquid phase. The equilibrium studies were also carried out using methanol as a solvent.

The sorption kinetic studies were conducted in a 100 cm^3 cylindrical glass vessel. An aqueous solution of DMP of 0.25 mol/dm^3 concentration at pH 10.5 was taken in the vessel and a known quantity of resin was added to it. The suspension was agitated using a six-blade glass turbine impeller at a speed of 1000–1200 rpm. Our earlier studies on sorption of acetic acid into weakly basic resins had indicated that at these speeds of agitation, the external film resistance is negligible (12). Samples were withdrawn from the suspension at regular time intervals and analyzed for the residual amine concentration.

Adsorption Column Studies

Column adsorption run was carried out by pumping an aqueous solution of DMP (0.25 mol/dm^3) through a 1.35 cm ID glass column packed with resins with the bed height of 0.2 m. The upward flow of the solution was selected to minimize channeling within the bed. The solution was pumped with a high-pressure duel reciprocating pump with a flow rate of 3 cm^3/min. Samples were withdrawn from the outlet stream at frequent time intervals. The adsorption run was continued until the outlet amine concentration became equal to the inlet amine concentration. The adsorption run was followed by desorption by methanol at the same flow rate followed by water wash to regenerate the resin bed.

RESULTS AND DISCUSSION

Equilibrium Studies

DMP being a weak base (pKa 9.6) can be present in ionic form to some extent, in the aqueous solution. Hence the possibility of ionic interaction between protonated amine species, if any, and the dissociated acidic functional group of the ion-exchange resin can not be completely neglected. To consider the ionic sorption, a reversible sorption model (13), is extended to describe the sorption behavior of the protonated amine in the ion-exchange resins. For convenience, the following abbreviations are used in the equations: $[N]$ for the amine; $[NH^+]$ for the protonated amine; $[R^-NH^+]$ for the amine complex with the resin's functional group and $[R^-]$ for the dissociated acidic functional group of the resin. Subscripts "S" and "L" denote solid and liquid phases, respectively.The complexation of the amine with the resin can be described by the following reaction:

$$\begin{tikzcd} {[N]_L + [RH]_S} \arrow[r, Leftrightarrow, "K_1"] \arrow[d, Leftrightarrow, "K."] & {[R^-NH^+]_S} \\ {[NH^+]_L + [R^-]_S} \arrow[r, Leftrightarrow, "K_2"] & {[R^-NH^+]_S} \end{tikzcd}$$

where, constants K_1 and K_2 are the measures of extent of interaction of molecular and protonated forms of the amine with the resin's acidic sites, respectively.K_1 and K_2 can be expressed as,

$$K_1 = \frac{[N]_L[RH]_S}{[R^-NH^+]_S} \tag{1}$$

$$\therefore [R^-NH^+]_S = \frac{[N]_L[RH]_S}{K_1} \tag{2}$$

$$K_2 = \frac{[NH^+]_L[R^-]_S}{[R^-NH^+]_S} \tag{3}$$

$$\therefore [R^-] = \frac{K_2[R^-NH^+]_S}{[NH^+]_L} \tag{4}$$

also,

$$K_a = \frac{[N]_L[H^+]_L}{[NH^+]_L} \tag{5}$$

$$\therefore [NH^+] = \frac{[N]_L[H^+]_L}{K_a} \tag{6}$$

If Q is the total capacity of the resin, then it can be given as,

$$Q = [R^-NH^+]_S + [R^-]_S + [RH]_S \tag{7}$$

Total amine concentration in the liquid phase (N_{LT}) can be given as,

$$N_{LT} = [N]_L + [NH^+]_L \tag{8}$$

from Eq (6)

$$N_{LT} = [N]_L + \frac{[N]_L[H^+]}{K_a} \tag{9}$$

$$\therefore N_{LT} = [N]_L\left\{1 + \frac{[H^+]}{K_a}\right\} \tag{10}$$

substituting Eq (2) and Eq (4) in Eq (7)

$$Q = \frac{[N]_L[RH]_S}{K_1} + \frac{K_2}{[NH^+]_L}\frac{[N]_L[RH]_S}{K_1} + [RH]_S \tag{11}$$

$$\therefore [RH]_S = \frac{Q}{\left\{([N]_L/K_1) + (K_2K_a/K_1[H^+]_L) + 1\right\}} = \frac{Q}{\left\{([N]_L/K_1) + K'\right\}} \tag{12}$$

where,

$$K' = 1 + \frac{K_2K_a}{K_1[H^+]_L} \tag{13}$$

substituting Eq (12) in Eq (2)

$$[R^-NH^+]_S = \frac{[N]_L[RH]_S}{K_1} = \frac{[N]_LQ}{K_1\left\{([N]_L/K_1) + K'\right\}} \tag{14}$$

$$\therefore [R^-NH^+]_S = \frac{[N]_LQ}{\{[N]_L + K_1K'\}} \tag{15}$$

Now, from Eq (6) and (13)

$$K' = 1 + \frac{K_2}{K_1}\frac{[N]_L}{[NH^+]_L} \tag{16}$$

$$\therefore [R^-NH^+]_S = \frac{[N]_LQ}{\left\{[N]_L + K_1\left(1 + (K_2/K_1)([N]_L/[NH^+]_L)\right)\right\}} \tag{17}$$

$$\therefore \left(\frac{Q[NH^+]_L}{[R^-NH^+]_S} - [NH^+]_L\right) = K_1\frac{[NH^+]_L}{[N]_L} + K_2 \tag{18}$$

From Eq (15), the value of Q can be calculated from the Y-intercept of the graph of $1/[R^-\mathrm{NH}^+]$ *vs* $1/[N]_L$. This Q value is then used in Eq (18) to get the values of K_1 and K_2. The slope and intercept of the plot of RHS of Eq (18) *vs* $[NH^+]_L/[N]_L$ give the values of K_1 and K_2, respectively. The values reported in Table 2 for Indion-652 and Indion-190 resins show that K_1 is greater than K_2 by an order of magnitude for weakly acidic resin, which indicates a comparatively smaller contribution of the ionic sorption to the total sorption of the amine. The sorption of the molecular amine is considered to be the primary mechanism of its sorption onto the resins.

Table 2. Regressed values of Q, K_1 and K_2

	Indion-652			Indion-190		
Temp.(K)	Q (mol/dm^3)	K_1 (mol/dm^3) $\times 10^2$	K_2 (mol/dm^3) $\times 10^3$	Q (mol/dm^3)	K_1 (mol/dm^3) $\times 10^2$	K_2 (mol/dm^3) $\times 10^3$
303	4.7	2.7	1.0	2.1	1.4	0.3
308	4.5	1.8	0.8	2.0	1.1	0.2
313	4.3	1.1	0.6	1.9	0.9	0.1
323	4.0	0.6	0.3	1.6	0.3	0.08

The adsorption capacity of the resin can be empirically correlated in terms of θ by Langmuir type isotherm,

$$\theta = \frac{K[N]_L}{1 + K[N]_L} \tag{19}$$

from Eq (6)

$$\theta = \frac{KN_{LT}/\left(1 + [H^+]/K_q\right)}{1 + KN_{LT}/(1 + [H^+]/K_a)} \tag{20}$$

$$\therefore \theta = \frac{q}{q_{\max}} = \frac{K'N_{LT}}{1 + K'N_{LT}} \tag{21}$$

Where q is the loading of the resin expressed as moles of DMP adsorbed per kg of dry resin, q_{max} is the maximum loading capacity and K' is the equilibrium constant and is a quantitative measure of the interaction between the amine and the resin. Figure 1 shows adsorbed amounts of DMP on three resins, Indion-652, Indion-190 and NPA-I, respectively. The adsorption increases rapidly at low amine concentrations and approaches a limiting value at higher DMP concentrations. The lines shown in Fig. 1 are the curves obtained by fitting the adsorption data into the Langmuir isotherm equation. The fitted values of K' and q_{max} are reported in Table 3 for the three resins. K' is the highest for the weak cationic exchange Indion-652 resin, while the nonionic polymeric adsorbent gave the poorest adsorption of the amine. The stronger acidic resin Indion-190 surprisingly showed poorer interaction than the weakly acidic resin. The difference in the sorption properties may be, therefore, strongly influenced by the functional group and structure of the resin. The capacity of a resin to adsorb a solute depends on the exchange capacity of the resin. For the strongly acidic Indion-190 resin the adsorption capacity is lower due to a lesser number of sites present in the resin (1.9 meq/gm) as compared to weakly acidic resin Indion-652 (3.5 meq/gm). The resin showed significant swelling in the aqueous solutions which makes the resin volume easily accessible to

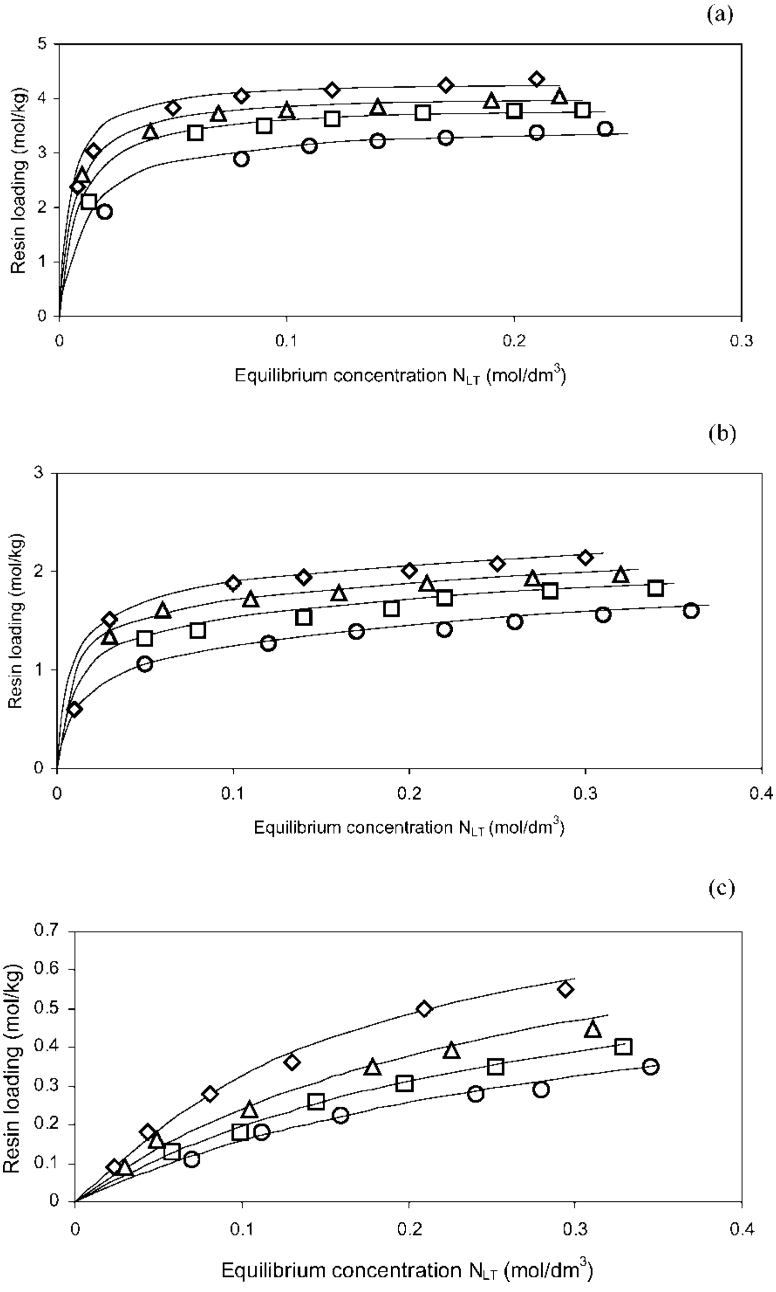

Figure 1. (a) Adsorption of DMP on Indion-652 at various temperatures: ◇: 303 K, △: 308 K, □: 313 K, ○: 323 K; (b) Adsorption of DMP on Indion-190 at various temperatures: ◇: 303 K, △: 308 K, □: 313 K, ○: 323 K; (c) Adsorption of DMP on NPA-I at various temperatures: ◇: 303 K, △: 308 K, □: 313 K, ○: 323 K.

Table 3. Langmuir adsorption isotherm parameters

		Indion-652			Indion-190			NPA-I		
Temp.(K)	Solvent	q_{max} (mol/kg)	K′ (dm^3/mol)	K_m (dm^3/mol)	q_{max} (mol/kg)	K′ (dm^3/mol)	K_m (dm^3/mol)	q_{max} (mol/kg)	K′ (dm^3/mol)	K_m (dm^3/mol)
303	Water	4.4	150	385	2.1	42	105	1.2	4.5	10.2
	Methanol	3.3	14.3	402	2.0	6.5	125	1.5	2.4	69
308	Water	4.1	124	288	2.0	35	87	0.9	3.6	8.3
313	Water	3.9	97	223	1.9	29	70	0.8	3.2	7.4
323	Water	3.6	69	171	1.7	23	56	0.7	2.9	6.7
ΔH kJ/mole		−40			−20.5			−18.1		

the solute. The tendency of the resin to swell, depending upon the degree of cross linking, was also more for Indion-652 resin than that for Indion-190 resin. The Indion-652 resin contains a lower percentage of the cross-linking and, therefore, swells to the greater extent. Indion-190 resin, however, being more cross- linked is relatively slow to the exchange of solute. Figure 2 shows the swelling ratio, defined as ratio of the resin volumes in swollen and dry states for the three resins. The swelling of Indion-652 resin increased with increasing DMP concentration. This could be due to relaxation of the polymer matrix to accommodate the amine complexation with the resin's acidic group. The amine after getting protonated by acidic hydrogen of the resin can remain associated with the anionic group of the resin. However, the protonated amine, because of its size, may not effectively

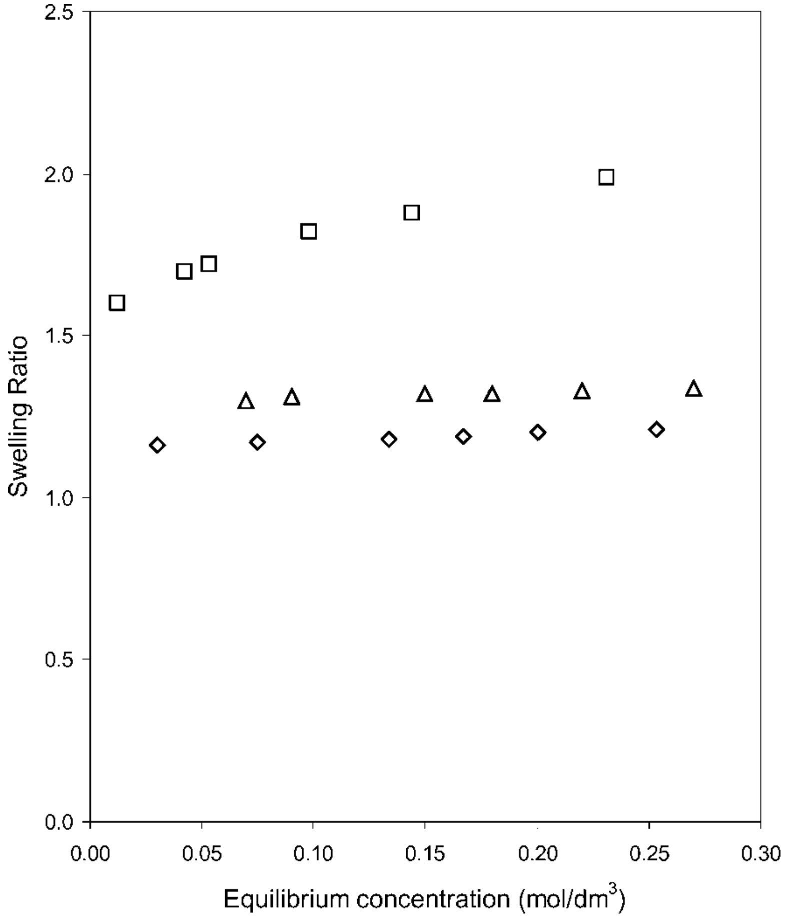

Figure 2. Swelling ration of resins in aqueous solution of DMP at 303 K: □: Indion-652, ◇: Indion-190, △: NPA-I.

neutralize the negative charge on the resin matrix. The presence of the solvent and partially neutralized charges on the resin matrix may force it to expand giving a higher swelling ratio (14). The adsorption of DMP on NPA-I is due to weaker van der Waals interactions as there is no reactive group present within the polymer matrix. Also its adsorption capacity for the amine is much lower than those of the acidic ion exchange resins.

The effect of temperature on the adsorption of DMP from aqueous solutions on all three resins is also evident in Fig. 1. The decrease in the adsorption of the amine with increase in temperature was expected, as adsorption is an exothermic process because of the entropy loss. The Langmuir adsorption constant and loading capacity, therefore, show a decreasing trend at higher temperatures (Table 3). The heats of adsorption can be estimated from the effect of temperature on the adsorption equilibrium constant by using the Van't Hoff equation.

$$\frac{d\ln(K)}{dT} = \frac{\Delta H^{\circ}}{RT^2} \tag{22}$$

The estimated values of ΔH are in the range of -15 to $-40\,\mathrm{kJ/mol}$ (Table 3). The heat of adsorption is a direct measure of the strength of the bonding between the surface adsorption site and the amine. The low values of ΔH show that the sorption of the amine is in the range of hydrogen bonding and no strong chemical interaction is responsible for the sorption.

To study the applicability of methanol as a desorbent, the equilibrium sorption studies were also carried out in methanol. The experimental data were fitted in Langmuir adsorption isotherm. The adsorption constant and loading capacity of the resins in methanol are also reported in Table 3. Figure 3 shows the experimental and fitted values of adsorption data in methanol using the three resins at 305 K. The equilibrium studies of DMP in methanol follow the same trend as that in water. The maximum interaction is found with Indion-652 resin followed by Indion-190 resin and NPA-I resin. However, the interaction of DMP with the resins in methanol is poorer than that in water. The poorer adsorption characteristics in methanol should permit its use as an effective desorbent.

The solvation of a solute in the solution phase also plays an important role in the sorption process. The adsorption has to compete with the relative interaction of the amine with the solvent in the solution. If a solute is preferably solvated by the solvent, its adsorption tendency becomes weaker while in the poorly solvated conditions the tendency to get adsorbed is stronger. The solvation of a solute in the liquid phase can be quantitatively estimated from its activity coefficient. If it is less than 1, the solvation is preferential, while if it exceeds 1, solvation of the solute in the solution phase decreases. The aqueous phase activity coefficient of DMP, as estimated by UNIFAC group contribution method (15), is in the range 0.4–0.44 in the concentration range studied in this work. The low value of activity coefficient of DMP

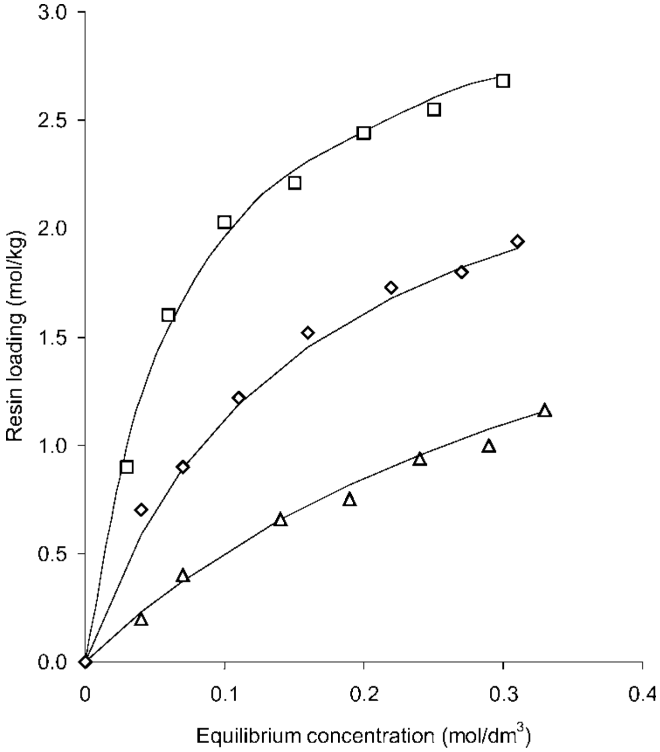

Figure 3. Adsorption of DMP on three resins from methanol at 303 K: □: Indion-652, ◇: Indion-190, △: NPA-I.

indicates the tendency of DMP to remain in the aqueous solution. It may be possible to include the activity coefficient (γ) of DMP to consider, as an approximation, the solvation effects on the adsorption in the resin. If the concentration terms in the Langmuir equation are replaced by the product of activity coefficient and concentration, then K_m should represent the specific interaction between the resin and the solute. The modified Langmuir isotherm is of the form,

$$\frac{q}{q_{\max}} = \frac{\gamma K_m N_{LT}}{1 + \gamma K_m N_{LT}} \tag{23}$$

The experimental sorption data were fitted in this modified isotherm. The modified K_m values are also given in Table 3. If the adsorption is solely influenced by solvation of solute in the solution, then K_m values should be the same or at least similar in two solvents. The trend in K_m values for different resins has remained the same as that of K_i' in water and methanol. The K_m values in water and methanol, particularly for Indion-652 and Indion-190 resins, are not the same but are now closer to each other indicating a better representation of the interaction of the amine with the acidic group.

Equilibrium Sorption Model

Langmuir isotherm does not consider the entire body of the polymer resin. It is based on the surface phenomenon and takes into account only the interaction of the solute with the functional groups. The simultaneous sorption of a solvent into the resin structure needs to be identified to ascertain the true sorption of the amine. If the sorption process is viewed as an equilibrium partitioning of the amine between the external aqueous phase and the swollen resin phase, the equilibrium can be analyzed by a thermodynamic model. The swollen resin phase is considered as a pseudo-homogeneous phase composed of the polymer, the solute and solvent and the amine is partitioned between this phase and an external solution, which does not include the polymer. The equilibrium is described by equating the activities of the involved components

$$a_i^p = a_i^l \tag{24}$$

where, *p* and *l* indicate polymer and the liquid phase respectively and *N* is the number of the components, excluding the polymer. The mass balance for the components can be written as:

$$n_i^p + n_i^l = n_i^0 \tag{25}$$

where, n_i is the number of moles of the *ith* component and the index *0* refers to the starting value. From these, we can compute the composition of the two phases, and the volume fractions v_i in the polymer phase as:

$$v_i = \frac{n_i^p V_i}{V_p^0 + \sum_{i=1}^{N} n_j^p v_j} \tag{26}$$

where, V_i is the molar volume of the *ith* component (115.3 cm^3/mol for DMP and 17.9 cm^3/mol for water). Vp^0 is the volume of the dry resins. The denominator of Eqn. 26 represents the total volume of the swollen polymer phase.

The activities in the swollen polymer phase can be evaluated using the extended Flory Huggins model (16).

$$\begin{aligned} lna_i^p = {} & 1 + lnv_i - \sum_{j=1}^{N+1} m_{ij} v_j + \sum_{j=1}^{N+1} \chi_{ij} v_j - \sum_{j=1}^{N+1} \sum_{k=1}^{j-1} m_{ik} v_j v_k \chi_{kj} \\ & + \eta v_i \left(\frac{5}{3} v_p^{1/3} - \frac{7}{6} v_p \right) \end{aligned} \tag{27}$$

where, the index $j = N + 1$ refers to the polymer, $Vp = V_{N+1}$ is the polymer volume fraction in the polymer phase and $m_{ij} = V_i/V_j$ is the ratio of molar volumes, χ_{ij} represents the molecular interaction between components i and j. The first three terms of the above equation account for the entropic contributions to the free energy of mixing, which is approximated by treating the system as a lattice with interchangeable polymer units and solvent molecules. The following two terms describe the energetic interactions among the molecules through the binary interaction parameters χ_{ij} and account for the enthalpy of mixing. The last term represents the elastic deformation contribution which is responsible for keeping the swelling of the resin finite (13).

The activity of DMP in the aqueous phase was evaluated using UNIFAC group contribution method (15). The interaction parameters (χ_{ij}) of the equilibrium sorption model were evaluated by fitting the experimental sorption data in the above equations using least square method. The negative values of interaction parameters indicate an attractive interaction whereas positive values show the repulsive tendency.

The fitted interaction parameters between DMP, water and the different resin at various temperatures are reported in Table 4. Figure 4 shows the fitted sorption data, as X^l-X^s plot representing mole fractions of DMP in two phases for various temperatures at equilibrium. The shifting of the plots towards the $X^l = X^s$ line, as the temperature increases, shows decrease in sorption efficiency with increase in temperature. The $X^l = X^s$ line represents the compositions at which the mole fractions of DMP in both, aqueous and resin phases, are equal. Plots above this line show that DMP is sorbed preferentially on the resins. The interaction parameters show that the interaction of DMP is the highest with the weakly acidic Indion-652 resin followed by Indion-190 resin and the least with the NPA-I resin. Water also shows some interaction with the resins (Table 4). However, as reflected from the interaction parameters, though water competes with DMP for the resin sites, it's interaction is insignificant.

Table 4. Interaction parameters (χ) of equilibrium sorption model

Temperature (K)	Indion-652		Indion-190		NPA-I	
	DMP	Water	DMP	Water	DMP	Water
303	−14.3	−1.0	−9.3	−0.2	−3.8	−0.1
308	−12.5	−0.6	−6.9	−0.09	−1.9	−0.04
313	−7.9	−0.2	−3.2	−0.03	−0.3	0.0
323	−3.3	−0.01	−0.9	0.0	−0.1	0.03

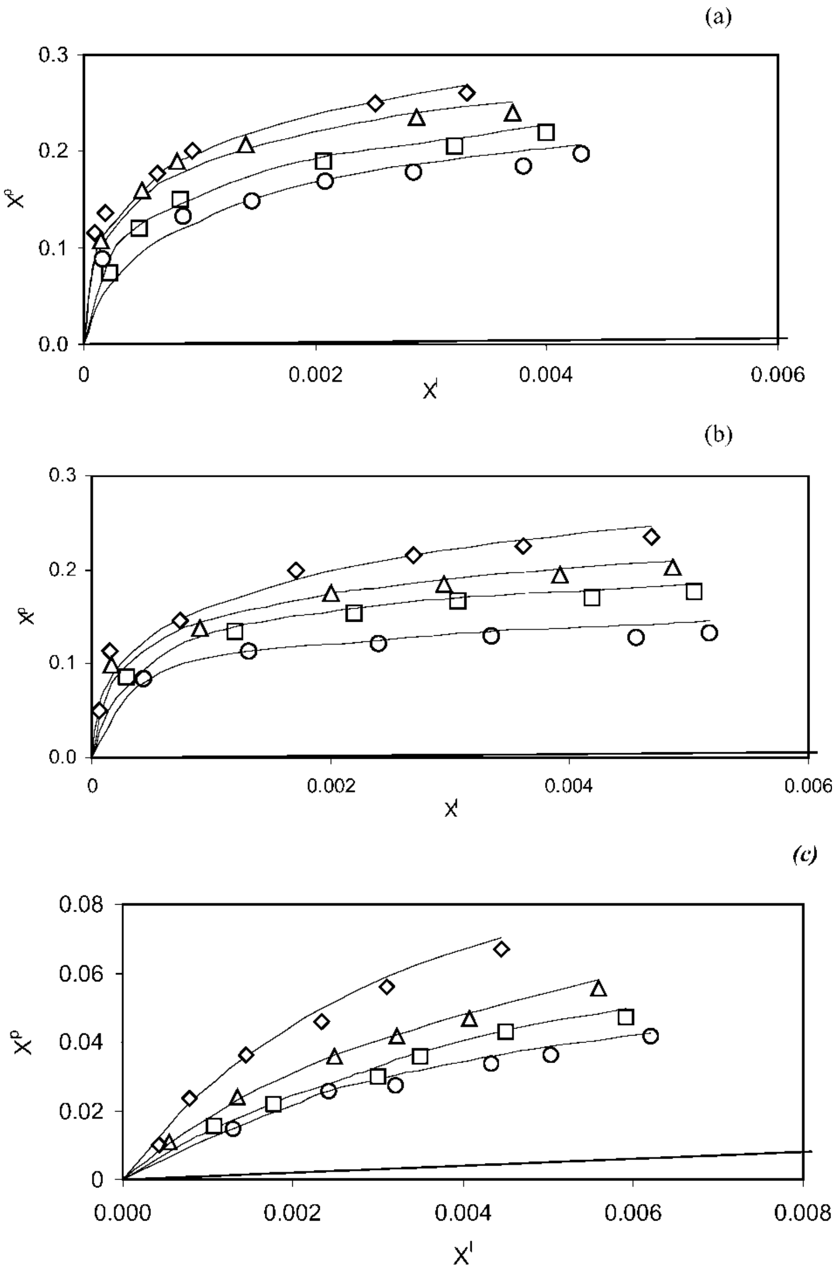

Figure 4. (a) Equilibrium sorption data for DMP on Indion-652 at various temperatures: ◇: 303 K, △: 308 K, □: 313 K; ○: 323 K; (b) Equilibrium sorption data for DMP on Indion-190 at various temperatures: ◇: 303 K, △: 308 K, □: 313 K, ○: 323 K; (c) Equilibrium sorption data for DMP on NPA-I at various temperatures: ◇: 303 K, △: 308 K, □: 313 K, ○: 323 K.

Kinetic Studies in a Stirred Vessel

Several mechanisms have been proposed to describe internal mass transfer, such as pore diffusion, surface diffusion, or a combination of both. Since the adsorption of undissociated amine was observed to be the major mechanism of sorption, the transport of only undissociated species has been considered. We consider the whole adsorption process as a combination of diffusion and adsorption (12). First, the solute diffuses from the bulk liquid through a film of liquid surrounding the resin to the external surface area of the resin. Then it diffuses through the resin structure with simultaneous adsorption of the solute. The mass balance equations for the same are written as:

(a) Mass balance equation in the bulk liquid phase,

$$V_e\left[\frac{d[N]_L}{dt}\right] = k_{sl}a_p\Big[[N]_L - [N]_{i(R_p,t)}\Big] \tag{28}$$

(b) Mass balance within the particle at a distance r from the center of particle is,

$$-\frac{1}{r^2}\frac{d}{dr}\left[r^2 D_e\frac{d[N]_i}{dr}\right] = \varepsilon_i\left[\frac{d[N]_i}{dt}\right] + \rho_p(1-\varepsilon_i)\left[\frac{dq}{dt}\right] \tag{29}$$

(c) Mass balance in the resin phase assuming instantaneous local equilibrium at the active site; i.e. no resistance to actual adsorption,

$$\frac{dq}{dt} = \left(\frac{dq}{d[N]_i}\right)\left(\frac{d[N]_i}{dt}\right) \tag{30}$$

The adsorbed phase concentration (q) was approximated using the Langmuir adsorption isotherm (Eq (21).
The initial conditions are,

$$\text{at,}\quad t = 0;\quad [N]_{i(r,0)} = 0 \quad \text{and} \quad [N]_{L(0)} = [N]_{Lf} \tag{31}$$

the boundary conditions are,

$$\text{at,}\quad r = R_p \quad D_e\frac{d[N]_i}{dr}\bigg|_{r=R_p} = k_{sl}\Big[[N]_L - [N]_{i(R_p,t)}\Big] \tag{32}$$

$$\text{and,}\quad \text{at } r = 0 \quad \frac{d[N]_{i(0,t)}}{dr} = 0 \tag{33}$$

The external solid-liquid mass transfer coefficient (k_{sl}) was estimated from an empirical correlation given by Levin and Glastonbury (17) for the solid-liquid mass transfer in agitated slurry.

$$\frac{k_{sl}d_p}{D_m} = 2.0 + 0.47\left(\frac{\varepsilon d_p^4}{\nu_L}\right)^{0.21}\left(\frac{d_s}{d_t}\right)^{0.17}\left(\frac{\mu_L}{\rho_L D_m}\right)^{0.36} \tag{34}$$

The energy dissipation rate per unit weight of the solution (ε) was determined using Eq (35)

$$\varepsilon = \frac{N_p n^3 d_s^5}{M} \tag{35}$$

The liquid molecular diffusivity (D_m) in m^2/sec was evaluated from the Wilke-Chang correlation (18).

$$D_m = 7.4 \times 10^{-8}\frac{T(xM_B)^{0.5}}{\mu V_A^{0.6}} \tag{36}$$

The estimated value of D_m and k_{sl} are $9.7 \times 10^{-9}\ m^2/sec$ and 5.9×10^{-5} m/sec, respectively. The estimation of effective diffusivity (D_e) of the DMP into the resin matrix was done by fitting the experimental kinetic data in the model equations. The values of D_e for three resins are shown in Table 5. The continuous curves in Fig. 5 denote the fitted values from the model while the points represent the experimental values. The internal mass transfer coefficient (k_i) (for the particle size of 0.75×10^{-3} m) based on this diffusivity was estimated using the following correlation (19).

$$k_i = 5\frac{D_e}{R_p \tau} \tag{37}$$

The external mass transfer coefficient is of the order 10^{-5} m/sec while the internal mass transfer coefficient was found to be of the order 10^{-7} m/sec, which clearly indicates that the intraparticle diffusion is the controlling resistance for the adsorption of DMP into the resin phase. For a resin with the internal porosity close to 0.35–0.45, the estimated tortuosity ($\tau = \varepsilon_i D_m/D_e$) is found to be very high (Table 5). The pore size of the resin (25-40 nm) is much larger than the kinetic diameter of the DMP molecule (0.9 nm). Therefore, it should diffuse with the same ease through different resins under the usual effects of pore tortuosity and voidage. However, effective diffusivity of DMP is different in different resins. The D_e in Indion-652 resin is

Table 5. Diffusivities of DMP in aqueous solution and tortuosity values in three resins

Resin	Indion-652	Indion-190	NPA-I
Effective diffusivity(m^2/s) $\times 10^9$	0.62	0.31	0.14
τ	7.2	12.6	26.2
Surface diffusivity(m^2/s) $\times 10^{12}$	0.7	1.46	25.9

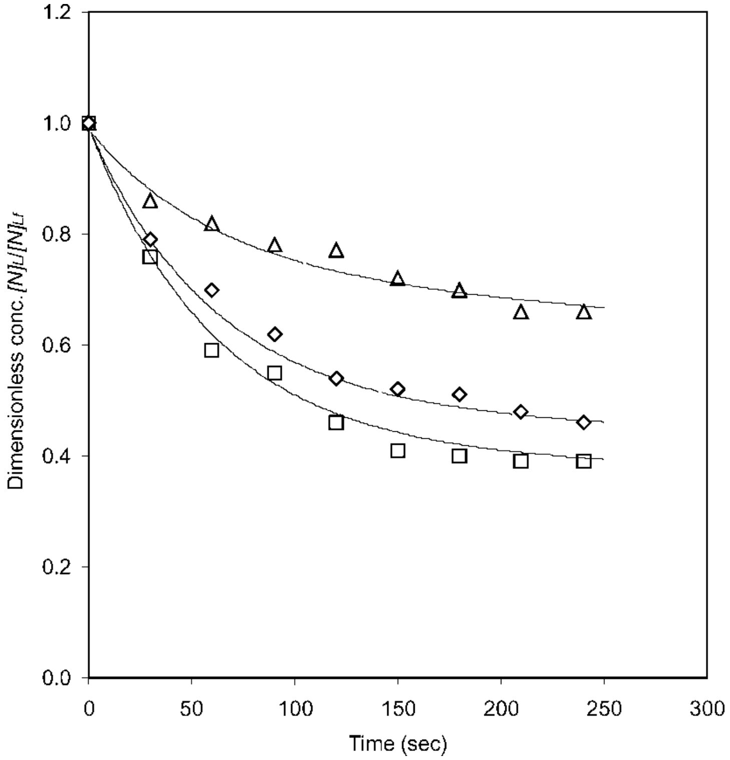

Figure 5. Kinetics of adsorption of DMP on Indion-652: □: Indion-652, ◇: Indion-190, △: NPA-I.

higher than that in Indion-190 and the least in NPA-I. This may be due to the different extent to which these resins swell. The maximum swelling is exhibited by Indion-652 resin. Due to the resin swelling, the penetration of the solute into the resin structure is facilitated. The sites are more easily accessible to the amine in a swollen resin than in non-swollen resin beads. Thus, the difference in the swelling characteristics of the resins probably accounts for the different effective diffusivities in the resins.

The variation in effective diffusivity in different resins may also indicate surface diffusion as an additional mode of mass transfer. If surface diffusion over the polymeric network contributes to the mass transfer in the resin phase, then the effective diffusivity is influenced by the adsorbed concentration. If the mass transfer is considered to be a combination of pore and surface diffusion, then the effective diffusivity can be expressed as a combination of pore diffusion and surface diffusivity terms (Eqn 38) (12).

$$D_e = D_{pore} + \frac{q_{\max} K'}{\rho} D_{surface} \tag{38}$$

The terms $q_{\max}$ and K' indicate the saturation capacity and Langmuir adsorption constant of the system under consideration. The pore diffusivity can be approximated for the usual range of the tortuosity factor of $\sim 1.5-2.0$ ($D_{pore} = \varepsilon_i D_m/\tau$). Using the above correlation, the surface diffusivity ($D_{surface}$) can be estimated from experimental D_e. This value was found to be higher for NPA-I and those for Indion-190 and Indion-652 resins are similar in magnitude (Table 5). These results, however, suggest that neither surface nor pore diffusion can be considered to be solely responsible for the migration of DMP through the polymeric network of the resin bead. Since effective diffusivity is expected to be higher with higher adsorbed phase concentration, which indeed is in accordance with the experimental observations, the contribution by surface diffusion seems to be significant.

Column Studies

To investigate further the applicability of the adsorption process for the recovery of DMP, column adsorption studies were conducted with an industrial mixture of DMP in water. Figure 6(a) shows dimensionless concentration of DMP in the effluent from the column versus the number of bed volumes of the solution passed through the column for Indion-652 resin. About 3 bed volumes of the feed solution were required to reach the breakpoint. At the break point, complete bed capacity had not been used, and the sorption efficiency of the resin bed was 66%. For the feed concentration of $0.25\,\mathrm{mol/dm^3}$, the loading capacity of the resin was expected to be 4.4 mol/kg resin. On complete saturation of the bed, for which additional 4 bed volumes were required, the bed showed a capacity of 4.3 mol/kg resin. This amount matches well with that expected from the equilibrium studies.

The regeneration of the loaded adsorbent and the recovery of the DMP is also an important objective. The elution of DMP was done with methanol because of the ease of the separation of methanol by distillation from the resulting solution. The regeneration curves are shown in Fig. 6(b). Almost 80% of the adsorbed DMP was eluted by 6 bed volumes of methanol at 30°C. Passing hot methanol through the bed enhances the elution process. About 96% of the adsorbed material was eluted from the column by treatment with 4 bed volumes of methanol at 50°C. The temperature effect can be, therefore, used advantageously for desorption. The same column was used for all the column runs after regeneration by alcohol followed by water wash each time which indicates the regenerability of the resin without loss of any capacity.

The dynamic behavior of the adsorption column was also modeled using the equilibrium and kinetic data. A linear driving force model based on external mass transfer and intraparticle diffusion was used to predict the breakthrough profiles (20). The numerical complexities involved in

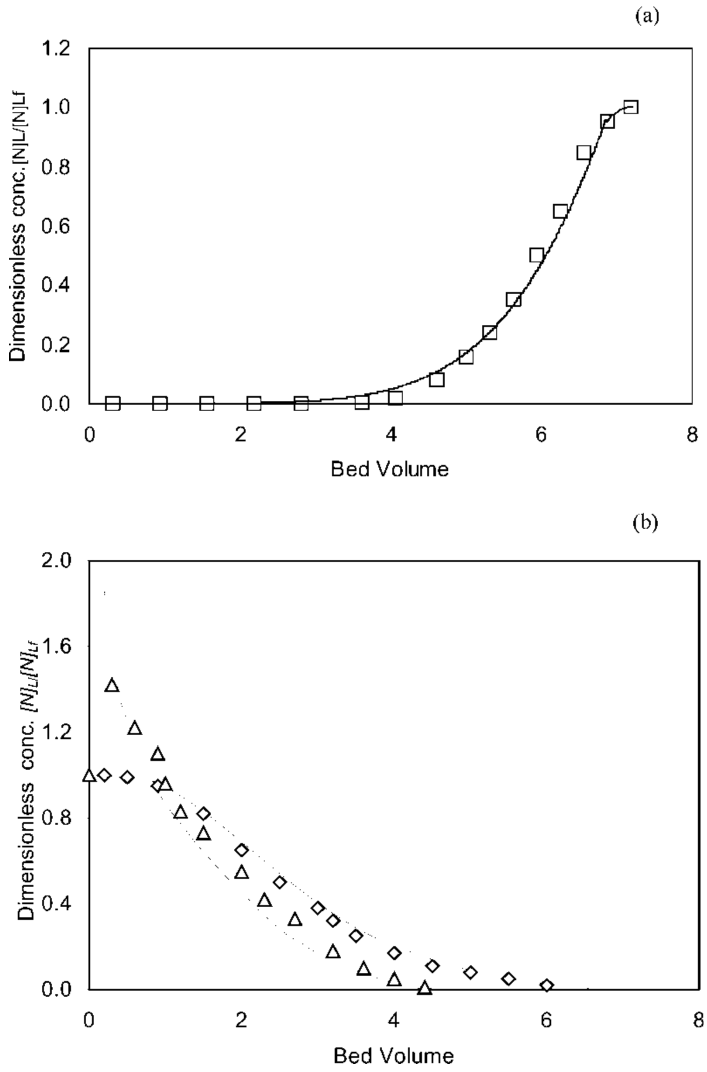

Figure 6. (a) Breakthrough curve for adsorption of DMP in fixed bed column on Indion-652; (b) Desorption of DMP from resin by Methanol: ◇: 303 K, □: 323 K.

the solution of the model were overcome by using a lumped parameter model so that the intraparticle concentration $[N]_i(r,t)$, becomes only a function of time; i.e. volume average concentration

$[N]_i(r,t)$ is defined as follows:

$$[N]_i(t) = \frac{1}{V_p}\int_{V_p} [N]_i(r, t)dV \tag{39}$$

The model equations are as follows:

(a) Mass balance in the external liquid phase,

$$\varepsilon_e \frac{d[N]_L}{dt} + u\frac{d[N]_L}{dz} - D_L\varepsilon_e \frac{d^2[N]_L}{dz^2} = -K_L\frac{3}{R_p}(1-\varepsilon_e)([N]_L - [N]_{i(Rp)}) \tag{40}$$

(b) Mass balance in the internal liquid phase (i.e., within the adsorbent particle),

$$\varepsilon_i \frac{d[N]_i}{dt} = K_L\frac{3}{R_p}([N]_L - [N]_i) - (1-\varepsilon_i)\rho_p\frac{dq}{dt} \tag{41}$$

(c) Mass balance in the adsorbed phase with equilibrium at the local level

$$\frac{dq}{dt} = \left(\frac{dq}{d[N]_i}\right)\left(\frac{d[N]_i}{dt}\right) \tag{42}$$

This set of equations was solved numerically using an explicit finite difference method. The derivatives terms in the above set of equations were approximated by difference terms and the resultant set of equations were solved numerically by appropriately adjusting the step size in z and t. The predicted values are represented by continuous curve in Fig. 6(a).

The value of the external mass transfer coefficient (k_{sl}) was estimated from the empirical correlation valid for low Reynolds number ($Re < 50$) in a packed bed (21).

$$k_{sl} = 1.85R_e^{-2/3}Sc^{-2/3}\left(\frac{u}{\varepsilon}\right)\left(\frac{1-\varepsilon}{\varepsilon}\right)^{-1/3} \tag{43}$$

where,

$$R_e = \frac{ud_p\rho_L}{6\mu(1-\varepsilon_e)\varepsilon_i} \tag{44}$$

$$S_c = \frac{\mu}{\rho_L D_m} \tag{45}$$

The estimated external mass transfer coefficient (k_{sl}) was 1.28×10^{-5} m/s. The internal mass transfer coefficient (k_i) was estimated using a correlation based on the effective diffusivity (D_e) in the particle and the tortuosity factor (eq 37). The overall mass transfer coefficient, K_L, was obtained from

$$\frac{1}{K_L} = \frac{1}{k_{sl}} + \frac{1}{k_i\varepsilon_i} \tag{46}$$

The dispersion coefficient (D_L) of the column can be estimated using the empirical correlation (22),

$$\varepsilon_e P_e = 0.2 + 0.011 R_e^{0.48} \tag{47}$$

where,

$$P_e = \frac{u d_p}{\varepsilon_e D_L} \tag{48}$$

$$R_e = \frac{u d_p \rho_L}{\mu \varepsilon_e} \tag{49}$$

The predicted curves (Figs.6 (a) and (b)) match well with the experimental data. Therefore, the dynamic behavior of the adsorption column can be successfully predicted.

CONCLUSION

The recovery of DMP can be carried out from aqueous solutions with cation exchange and nonionic polymeric resins. Adsorption of undissociated amine contributes mainly to the sorption of DMP from aqueous solutions on acidic ion-exchange resins. The uptake of DMP by a resin is highly influenced by the structure of the resin. It could be desirable to use weakly acidic cation exchange resin in view of its favorable isotherms higher capacity and easy regenerability. Adsorption of DMP is controlled by intraparticle diffusion into the resin phase. It was established from the column studies that the recovery of DMP can be successfully carried out by adsorption on ion-exchange resin; desorption being effectively carried out using methanol at higher temperatures. The dynamic behavior of adsorption column was modeled using the equilibrium and kinetic data. Predicted breakthrough curves agree well with experimental ones.

NOMENCLATURE

a_i	activity of component i
a_p	total area of the particle (m^2)
De	effective diffusivity (m^2/s)
D_L	dispersion coefficient (m^2/s)
D_m	molecular diffusivity (m^2/s)
D_{pore}	pore diffusivity
$D_{surface}$	surface diffusivity (m^2/s)
d_p	particle diameter (m)
d_s	diameter of the turbine (m)

d_t	diameter of the tank (m)
K'	Langmuir adsorption equilibrium constant (dm^3/mol)
K_m	modified Langmuir adsorption equilibrium constant (dm^3/mol)
k_{sl}	external solid-liquid mass transfer coefficient (m/s)
k_i	internal mass transfer coefficient (m/s)
M	mass of the reaction fluid (kg)
M_B	solvent molecular weight
n	speed of agitation (rps)
N_p	power number (5.2 for the 6-bladed turbine)
N_{LT}	total DMP concentration (mol/dm^3)
$[N]$	Concentration of molecular DMP (mol/dm^3)
$[NH^+]$	concentration of protonated amine species (mol/dm^3)
$[R^-NH^+]$	concentration of amine complex with the resin site (mol/dm^3)
$[N]_i$	concentration of DMP in the internal liquid phase (mol/dm^3)
Q	capacity of the resin (mol/dm^3)
q	adsorption capacity (mol/kg of resin)
q_{max}	maximum adsorption capacity (mol/kg of resin)
R_p	particle radius (m)
R_e	Reynolds number
S_c	Schmidt number
T	temperature (K)
t	time (s)
u	superficial velocity (m/s)
V_A	molal volume of DMP at normal boiling point (m^3/kmol)
V_p	volume of packed bed (m^3)
V_o	volume of external phase (m^3)
x	association parameter (2.6 for water)
z	bed height (m)

Greek Symbols

γ	activity coefficient
ρ	liquid density (kg/m^3)
ρ_p	particle density (kg/m^3)
ε_i	pore voidage
ε_e	bed voidage
ε	energy dissipation rate per unit weight of the solution (as defined by Eq 35)
θ	dimensionless resin phase concentration (as defined by Eq 19)
η	elasticity parameter (mol/cm^3)
τ	tortuosity factor

μ	viscosity of liquid (kg/m.s)
ν_L	kinematic viscosity of the liquid (m^2/sec)

REFERENCES

1. Pradip, K.P. and Sharma, M.M. (1991) Recovery of heterocyclic amines from dilute aqueous waste streams. *Ind. Eng. Chem. Res.*, 30: 1886.
2. Radeke, K.H. (1985) Adsorption method for treating wastewater. Ger. Pat. 2,12,028*cf Chem. Abstr.,* 102, 100325.
3. Gyunter, L.I., Shatalaev, I.F., and Bakulin, N.D. (1983) Evaluation of the toxicity of compounds of wastewaters from petrochemical production. *Vodosnabzh. Sanit. Tekh*, 7: 26; *cf Chem., Abstr.*1977, 86, 21391.
4. Nikolenko, N.V., Nechaev, E.A., and Pavlyuchik, G.S. (1988) Some principles of selection of sorbents for purification of sewage. *Kolloids*, 48: 823*cf Chem. Abstr.*1986, 105, 177839.
5. Cech, S. and Chudoba, J. (1987) Effect of activated sludge on the rate of removal of organic substances and their bidegradibility. *Vodni Hospad B*, 37 (2): 40; *cf Chem. Abstr.,* 1987, 106, 201184.
6. Kaczvinsky, J., Saitoh, K., and Fritz, J. (1983) Cation exchange concentration of basic organic compounds from aqueous solution. *Anal. Chem.*, 55: 1210.
7. Deshmukh, S. W, Pangarkar, V.G. (1984) Recovery of organic chemicals from effluents by adsorption over polymeric adsorbents. *Ind. Chem. Engg.*, 26 (3): 35.
8. Martin, R.J. and Iwugo, K.O. (1982) Recovery of α-picoline from water by the activated carbon adsorption process. *Stud. Environ. Sci.*, 19: 435.
9. Crooke, E.H. and McNulty, J.T. (1959) Removal and recovery of phenols from industrial waste effluents with amberlite XAD polymeric adsorbent. *Ind. Eng. Chem. Prod. Res. Dev.*, 14 (2): 113.
10. Budde, F. Frederik, J. (1990) Extractive recovery of ethylene amines. Eur. Pat. Appl. EP 367,312; *cf Chem. Abstr.*, 113, 134626.
11. Perrin, D.D. (1965) *Dissociation Constants of Organic Bases in Aqueous Solution*.
12. Anasthas, H.M. and Gaikar, V.G. (2001) Removal of acetic acid impurities from ethyl acetate by adsorption on ion exchange resins. *Sep. Sci. Technol.*, 36 (12): 2623.
13. Bhandari, V.M., Juvekar, V.A., and Patwardhan, S.R. (1992) Sorption studies on ion exchange resins. 2. Sorption of weak acids on weak base resins. *Ind. Eng. Chem. Res.*, 31: 1073.
14. Anasthas, H.M. and Gaikar, V.G. (2001) Adsorption of acetic acid on ion-exchange resins in non-aqueous conditions. *React. Funct. Poly*, 47 (1): 23.
15. Fredenslund, A., Gmehling, J., and Rasmussen, P. (1977) *Vapor-Liquid Equilibria using UNIFAC*; Elsevier: Amsterdam, The Netherlands.
16. Flory, P.J. (1942) Thermodynamics of high polymer solutions. *J. Chem. Phys.*, 10: 619.
17. Levins, D.M. and Glastonbury, J.R. (1972) Particle-liquid hydrodynamics and mass transfer in a stirred vessel. Part 2-mass transfer. *Trans. Instn. Chem. Engrs.*, 50 (2): 132.
18. Wilke, C.R. and Chang, P. (1955) Correlation of diffusion coefficients in dilute solutions. *A.I. Ch. E.J.*, 1: 264.
19. Glueckauff, E. (1982) Part 10: Formulation for diffusion into spheres and their application to chromatography. *Trans. Faraday Soc.*, 21 (3): 446.

20. Carra, S., Santacesaria, E., Morbidelli, M., Servida, A., and Starti, G. (1982) Separtion of Xylenes on Y Zeolites. 2. Breakthrough Curves and Their Interpretation. *Ind. Eng. Chem. Process. Des. Dev*., 21 (3): 446.
21. Kataoka, T., Yoshida, H., and Ueyama, K. (1972) Mass transfer in laminar region between liquid and packing material surface in a packed bed. *J. Chem. Eng. Jpn.*, 5 (2): 132.
22. Butt, J.B. (1980) *Reaction Kinetics and Reactor Design*; Prentice Hall: Englewood Cliffs, NJ.